

Human Monocytes Exposed to SARS-CoV-2 Display Features of Innate Immune Memory Producing High Levels of CXCL10 upon Restimulation

Jelena Cvetkovic^a Ronald H.J. Jacobi^a Alberto Miranda-Bedate^a
Nhung Pham^{b,c} Martina Kutmon^c James Groot^a
Martijn D.B. van de Garde^a Elena Pinelli^a

^aCentre for Infectious Disease Control, National Institute for Public Health and the Environment (RIVM), Utrecht, The Netherlands; ^bDepartment of Bioinformatics – BiGCaT, NUTRIM, Maastricht University, Maastricht, The Netherlands; ^cMaastricht Centre for Systems Biology (MaCSBio), Maastricht University, Maastricht, The Netherlands

Keywords

Trained immunity · Severe acute respiratory syndrome coronavirus 2 · CXCL10 · Monocytes

Abstract

Introduction: A role for innate immune memory in protection during COVID-19 infection or vaccination has been recently reported. However, no study so far has shown whether the severe acute respiratory syndrome coronavirus 2 (SARS-CoV-2) can train innate immune cells. The aim of this study was to investigate whether this virus can induce trained immunity in human monocytes. **Methods:** Monocytes were exposed to inactivated SARS-CoV-2 (iSARS-CoV-2) for 24 h, followed by a resting period in the medium only and a secondary stimulation on day 6 after which the cytokine/chemokine and transcriptomic profiles were determined. **Results:** Compared to untrained cells, the iSARS-CoV-2-trained monocytes secreted significantly higher levels of IL-6, TNF- α , CXCL10, CXCL9, and CXCL11 upon restimulation. Transcriptome analysis of iSARS-CoV-2-trained monocytes revealed increased expression of several inflammatory genes. As epigenetic and metabolic

modifications are hallmarks of trained immunity, we analyzed the expression of genes related to these processes. Findings indicate that indeed SARS-CoV-2-trained monocytes show changes in the expression of genes involved in metabolic pathways including the tricarboxylic acid cycle, amino acid metabolism, and the expression of several epigenetic regulator genes. Using epigenetic inhibitors that block histone methyl and acetyltransferases, we observed that the capacity of monocytes to be trained by iSARS-CoV-2 was abolished. **Conclusion:** Overall, our findings indicate that iSARS-CoV-2 can induce properties associated with trained immunity in human monocytes. These results contribute to the knowledge required for improving vaccination strategies to prevent infectious diseases.

© 2023 The Author(s).
Published by S. Karger AG, Basel

Introduction

It is already more than 3 years since the World Health Organization declared the spread of coronavirus disease 2019 (COVID-19) caused by severe acute respiratory

syndrome coronavirus 2 (SARS-CoV-2) as a pandemic. Considering long-term side-effects for some individuals, breakthrough infections, and the decline of vaccine-induced immunity, it has become clear that a better understanding of the mechanisms underlining the immune response to this virus remains crucial. Many studies have already shown that individuals who had been previously infected with SARS-CoV-2 develop a natural immunity including a virus-specific antibody and T-cell response which provides protection against reinfection [1, 2]. However, not much is known about innate immunity induced by this virus, particularly whether SARS-CoV-2 could induce innate immune memory also referred to as “trained immunity.”

Until recently, immunological memory was ascribed as a hallmark of the adaptive but not of the innate immune system. However, during the past decade, there has been increasing body of evidence showing that innate immune cells can retain memory after a previous exposure to infectious agents or vaccines and can respond faster and stronger to subsequent infections [3–5]. Unlike adaptive immune memory, which is antigen-specific, innate immune memory is nonspecific as it can be triggered by re-encounter with different stimuli [3, 5]. The mechanisms that define and mediate trained immunity involve metabolic (increased glycolysis, tricarboxylic acid [TCA] cycle remodeling, alterations in cholesterol, fatty acid biosynthesis, and amino acid metabolism) and epigenetic rewiring (epigenetic modifications including histone acetylation and methylation) that enhances the innate immune response to secondary stimuli [6–10]. Previous studies have demonstrated that various pathogen-associated molecular patterns including β -glucan (part of the cell wall of *Candida albicans*), lipopolysaccharide (LPS), muramyl dipeptide (MDP), uric acid, and oxidized low-density lipoprotein [11–13], but also Bacillus Calmette-Guérin (BCG) vaccine, mumps, measles, rubella vaccine, as well as seasonal influenza vaccine could efficiently induce innate immune memory [4, 14–16].

COVID-19 vaccines have recently also been described to induce trained immunity. In humans, as well as in mice, booster vaccination with Pfizer-BioNTech COVID-19 mRNA vaccine (BNT162b2) showed increased innate antiviral immunity compared to primary vaccination [17, 18]. Furthermore, a single dose of the ChAdOx1 nCoV-19 vaccine (Astra-Zeneca) resulted in phenotypical changes in monocytes with enhanced proinflammatory functions up to several months after vaccination [19].

Recently, the immune-cell epigenomic landscape of peripheral blood mononuclear cells (PBMCs) from individuals recovering from COVID-19 revealed that

adaptive, but also innate, immune cells build up immune memory after infection, as indicated by reprogramming of chromatin accessibility [20]. Another study shows that monocytes isolated from acute COVID-19 patients displayed hyper-responsiveness after LPS stimulation compared to monocytes isolated from healthy individuals. In addition, monocytes from convalescent COVID-19 patients showed long-lasting epigenetic changes, which, according to the authors, indicate the induction of trained immunity in monocytes [21].

Although these studies have suggested that COVID-19 vaccination and infection could induce trained immunity, there are no studies so far showing that SARS-CoV-2 can directly train innate immune cells to respond stronger to a second stimulus. Therefore, we investigated whether this virus could induce trained immunity in human monocytes.

Material and Methods

Viral Culture, Preparation, and Characterization

The SARS-CoV-2 used in this study was originally isolated from a Dutch patient (hCoV-19/Netherlands/ZuidHolland_0133R/2020; SARS-CoV-2 Wuhan-D614G) in March 2020. Culture and isolation were performed using VERO E6 cells as previously described by Van de Ven et al. [22]. Prior to inactivation, the infectious viral particles were quantified in culture supernatant using TCID50 assay to be able to determine the multiplicity of infection (MOI). Inactivated SARS-CoV-2 (iSARS-CoV-2) stock was achieved by incubating the stock at 60°C for 2 h after which iSARS-CoV-2 was stored at –80°C.

A/California/07/2009 (H1N1) influenza virus was obtained from the National Institute for Biological Standards and Control (NIBSC, London, England). H1N1 was cultured as previously described by Van de Ven et al. [23]. Inactivated H1N1 (iH1N1) was obtained by incubating the virus at 60°C for 2 h after which iH1N1 was stored at –80°C. Endotoxin levels in iSARS-CoV-2 (MOI: 3, 1, 0.1) and iH1N1 (MOI: 3, 1, 0.1) were measured using Pierce™ Chromogenic Endotoxin Quant Kit (Thermo Scientific) and were lower than 0.5 EU/mL, the limit provided by the US Food and Drug Administration guidelines. Also, using human HEK-Blue™ hTLR4 cells (Invivogen), no endotoxin was detected in the iSARS-CoV-2 and iH1N1 preparations.

Isolation of Human Monocytes from PBMCs

Human monocytes were purified from the buffy coats from healthy donors. To this purpose, PBMCs were isolated using a Lymphoprep (Nycomed, Zurich, Switzerland) gradient. Monocytes were isolated by negative magnetic sorting from PBMC using a MojoSort™ Human CD14+Monocytes kit (BioLegend, San Diego, CA, USA) according to the manufacturer's instructions. Purity of isolated monocytes was determined using anti-CD14-PE (BD Biosciences) FACS-staining. Data were acquired using the FACSCanto II (BD Biosciences) and analyzed using FlowJo software (Tree Star). CD14+ cell purity of 90% or more was obtained for each donor.

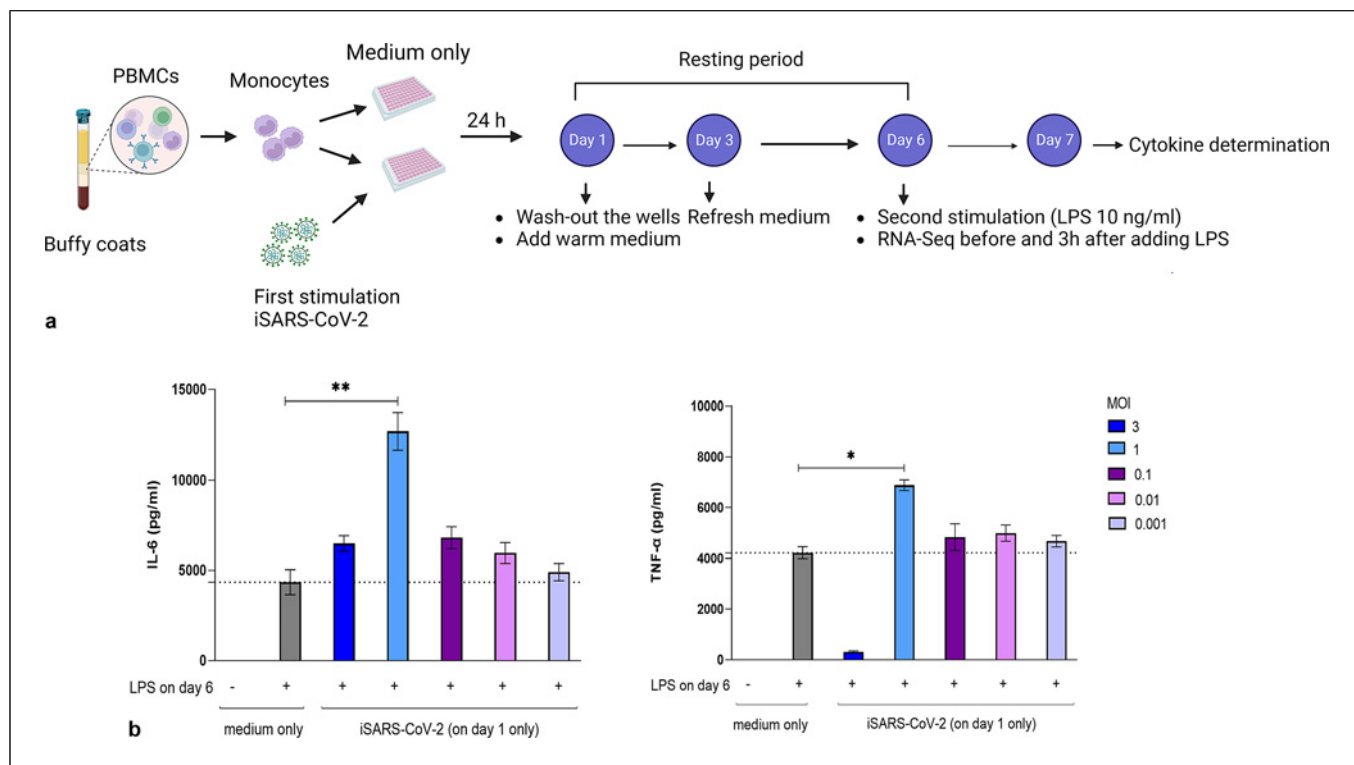


Fig. 1. Dose response of monocytes to inactivated SARS-CoV-2 at different MOI. **a** Schematic overview of the experimental design to induce trained immunity in human monocytes, created with Biorender.com. **b** Human monocytes were cultured in medium only or incubated with iSARS-CoV-2 (MOI: 3, 1, 0.1, 0.01, or 0.001) for 24 h after which the cells were washed and allowed to rest for 5 days. On day 6, the cells were stim-

ulated with LPS (10 ng/mL) and the secreted cytokines and chemokines were measured after 24 h. Kruskal-Wallis test followed by the Dunn's post hoc test was used to compare LPS-stimulated untrained monocytes and monocytes trained with iSARS-CoV-2 at MOI: 3, 1, 0.1, 0.01, or 0.001. Data are presented as the mean \pm SD from six donors ($n = 6$ from two independent experiments). * $p < 0.05$.

Culture and Training of Human Monocytes

Monocytes were cultured in a 24-well plate (4×10^5 cells/well) or 6-well plate (1×10^6 cells/well) in IMDM culture medium supplemented with 1% FCS, 100 units/mL penicillin, 100 μ g/mL streptomycin, and 29.2 μ g/ml L-glutamine (Gibco). Monocytes were exposed to iSARS-CoV-2 at different MOI (3, 1, 0.1, 0.01, or 0.001), iH1N1 (MOI: 3, 1, or 0.1), LPS (0.01 pg/mL), MDP (2 μ g/mL), or β -glucan (1 μ g/mL, all from Invivogen) to induce training or left in the medium only as untrained control. After 24 h incubation, cells were washed and allowed to rest for 5 days with a medium refreshing step on day 3 (shown in Fig. 1a). On day 6, cells received a secondary stimuli of either LPS (10 ng/mL) or inactivated *Bordetella pertussis* (MOI: 2) and incubated overnight. *B. pertussis* was inactivated at 60°C for 30 min. Culture supernatants were collected on day 7 and stored at -80°C for cytokine and chemokine quantification.

To evaluate the effects of iSARS-CoV-2 training on monocyte gene expression, the cells were cultured in a 6-well plate (1×10^6 cells/well) and trained as described above using a MOI: 1. On day 6, before or 3 h after LPS (10 ng/mL) stimulation, the cells were lysed in QIAzol (Qiagen) and stored at -80°C for subsequent RNA isolation.

Training experiments with histone acetylation and methylation inhibitors were performed as described above with the difference that monocytes were pretreated with 0.5 and 1 μ m histone acetyltransferase inhibitor C-646 (Abcam) or with 0.1 and 0.5 mM methyltransferase inhibitor 5'-Deoxy-5'-(methylthio) adenosine (MTA, Sigma-Aldrich). After 1 hour incubation with the inhibitors, the cells were trained with iSARS-CoV-2 (MOI: 1) for 24 h, followed by a washing step and allowing the cells to rest for 5 days as described above. On day 6, the cells were rechallenged with LPS (10 ng/mL) and the supernatants were collected 24 h later to determine cytokine and chemokine secretion.

Cytokine and Chemokine Analysis

Cytokines and chemokines were measured in culture supernatants using multiplex bead-based assays (LEGENDplex Human Inflammation, LEGENDplex Human Antivirus Response, and LEGENDplex HU Proinflammatory Chemokine Panel, BioLegend) to quantify secreted IL-1 β , IL-6, IL-10, IL-12p70, IFN- α 2, IFN- β , IFN- λ 1, IFN- λ 2/3, IFN- γ , TNF- α , GM-CSF, IL-17A, IL-18, IL-23, IL-33, CXCL1, CXCL8, CXCL9, CXCL10, CXCL11, CCL3, CCL4, CCL5, CCL11, CCL17, CCL20, and MCP-1. Data were

acquired using FACSCanto (BD Biosciences) and analyzed using Biolegend's Legendplex data analysis software. The results are expressed as pg/mL or as fold changed over medium control.

RNA-Seq Analysis and Data Processing

Total RNA was purified from the monocyte lysates using miRNeasy Mini Kit (Qiagen) following the manufacturer's instructions. Library preparation and RNA sequencing were performed as previously described by Kroes et al. [24]. More than 15 million reads were obtained and analyzed for each sample. FASTQ files coming from Illumina platform were merged, and quality controls were performed with FASTQC tools. FASTQ reads were aligned to the *Homo sapiens* reference genome (GRCh38), and transcript abundance was quantified using kallisto (version 0.46.1) [25]. Low count genes were filtered out and normalization of the data was performed using the EDAsq R package. RUVseq R package was used for correcting batch and donor effects.

Differential Gene Expression Analysis

The differentially expressed gene (DEG) lists were estimated using DeSeq2 R package under standard parameters. The groups: untrained (Unt-Med), untrained+LPS (Unt-LPS), trained with SARS-CoV-2 (Trn_S-Med), and trained with SARS-CoV-2+LPS (Trn_S-LPS) were used for the comparisons. For each comparison, genes were considered to be significantly DEGs if they obtained a p value (Benjamini-Hochberg multiple testing [padj]) lower than 0.05. Gene expression was visualized using the ComplexHeatmap-R package. A hierarchical cluster dendrogram was obtained by Ward's D2 method using Spearman correlation gene distances or K-means-supervised clustering. K was determined based on the number of groups involved in the analysis, e.g., Unt-Med, Unt-LPS, Trn_S-Med, and Trn_S-LPS.

Pathway Enrichment Analysis

Gene set enrichment analysis (GSEA) was performed with the fgsea R-package (v1.22.0) [26] to compare trained and untrained monocytes. All genes were ranked by the following formula: $-\log_{10}(\text{padj}) * \text{signed log}_2(\text{fold change})$. The ggplot2 R-package was used for the visualization of the results (version 3.4.1) [27].

GSEA was performed with the Hallmark gene set collection from the Molecular Signatures Database (MSigDB, version v2023.1.Hs) [28, 29] to study the affected processes between SARS-CoV-2-trained and -untrained monocytes without and with LPS stimulation. The normalized enrichment score and false discovery rate (<0.05) were calculated for each gene set using the Hallmark pathway database. To dive deeper into the metabolic rewiring in trained immunity, we also performed GSEA on a filtered collection of only metabolic pathways from the human pathway collection from WikiPathways (version 20210910) [30]. The data were visualized on altered metabolic pathways in Cytoscape [31] using the WikiPathways app [32].

Statistical Analysis

Using the Shapiro-Wilk test, we show that the cytokine and chemokine data did not follow a Gaussian distribution, therefore nonparametric testing was performed. The figure legends provide detailed information on the statistical tests applied and the number of individuals included in the analysis. The Wilcoxon-Mann-Whitney or Kruskal-Wallis tests were used depending on the number of groups compared. Wilcoxon-Mann-Whitney test was performed for the comparison of two groups and all the p values

were corrected by the Benjamini-Hochberg test in R. Effect sizes (ESs) calculated as Cliff's delta [33] were applied as previously described by Kroes et al. [24]. ESs were categorized into small <0.28 ; medium, <0.43 ; large, <0.7 ; and very large ≥ 7 according to Vargha and Delaney [34]. Comparisons with both $p < 0.05$ and ES either medium or larger are considered statistically significantly different, whereas $p < 0.1$ and ES either large or very large and $p < 0.15$ and ES very large are considered biologically significantly different. Kruskal-Wallis test was performed for multiple comparisons followed by Dunn's as post hoc test (using GraphPad Prism version 9.51 for Windows, GraphPad Software, San Diego, CA, USA). Data are presented as the mean \pm SD, and differences were considered significant at $p < 0.05$.

Results

iSARS-CoV-2 Trains Human Monocytes to Secrete Higher Levels of Cytokines and Chemokines Following a Secondary Stimulation

To investigate whether direct interaction between SARS-CoV-2 and monocytes can result in trained immunity, we incubated monocytes isolated from 6 healthy donors for 24 h with the inactivated viral preparation (iSARS-CoV-2) at different MOI. After washing out the first stimulus, the cells were cultured further for several days. On day 6, the iSARS-CoV-2 exposed and unexposed cells were incubated with a secondary LPS (10 ng/mL) stimulus followed by cytokine determination in the culture supernatant after overnight incubation (shown in Fig. 1a). Monocytes with prior iSARS-CoV-2 exposure to MOI: 1, but not to higher or lower MOI, produced significantly higher levels of IL-6 and TNF- α compared to unexposed monocytes (shown in Fig. 1b). Enhanced cytokine production after the second stimulation implies that iSARS-CoV-2, specifically at MOI: 1, induced trained immunity in human monocytes. Next, we confirmed and extended these findings by training monocytes from 12 healthy donors with iSARS-CoV-2 MOI: 1 and by using broader cytokine/chemokine determination after secondary LPS stimulation. Our in vitro model for inducing iSARS-CoV-2 training again showed significantly higher levels of IL-6 (1.7-fold increase), TNF- α (1.7-fold increase), and in addition significantly higher levels of CXCL10 (4-fold increase), CXCL9 (1.4-fold increase), and CXCL11 (1.5 fold-increase), as well as a trend toward increased levels of IL-10 when compared to the untrained cells incubated with LPS (shown in Fig. 2). The levels of CXCL8 and CCL5 secreted by the iSARS-CoV-2-trained cells were not significantly different to those of the unexposed cells after LPS stimulation, and the levels of IL-1 β , IL-12p70, IFN- α 2, IFN- β , IFN- λ 1, IFN- λ 2/3, IFN- γ , GM-CSF, IL-17A, IL-18, IL-23, IL-33, CXCL1, CCL3,

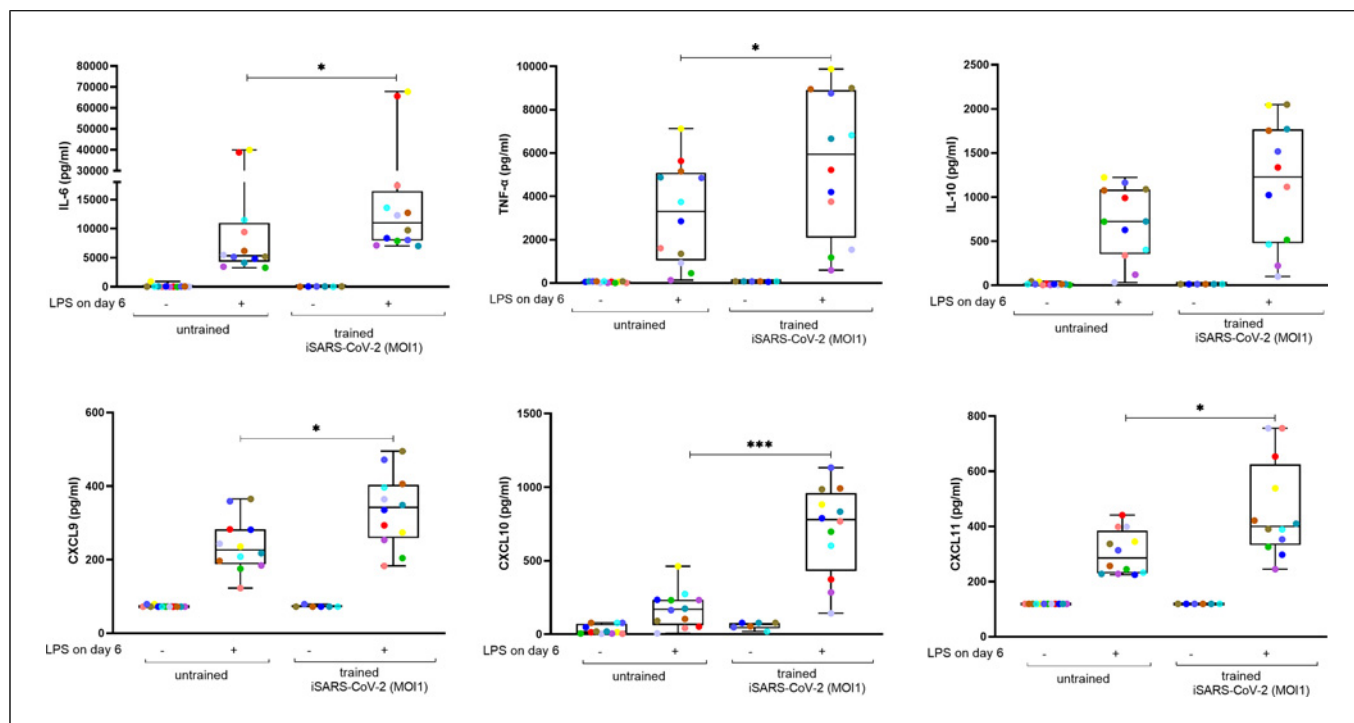


Fig. 2. Training of monocytes with iSARS-CoV-2 (MOI: 1). Human monocytes were cultured in medium only or exposed to iSARS-CoV-2 (MOI: 1) for 24 h after which the cells were washed and fresh culture medium was added. The cells were further incubated for 5 days and then stimulated with LPS (10 ng/mL) on day 6. After 24 h incubation, cytokine and chemokine secretion

were determined. Cells cultured in medium only or cultured in medium and stimulated with LPS on day 6 were used as controls. Two groups were compared using Wilcoxon-Mann-Whitney test (LPS-stimulated untrained monocytes with iSARS-CoV-2-trained monocytes). The results are expressed as the mean \pm SD ($n = 12$ from five independent experiments). * $p < 0.05$; *** $p < 0.001$.

CCL4, CCL11, CCL17, CCL20, and MCP-1 were not significantly different to those of the unexposed cells in the medium only (data not shown)."

To validate our in vitro model for the induction of trained immunity in monocytes, we also exposed these cells to either β -glucan (1 μ g/mL), MDP (2 ng/mL), or low concentration of LPS (0.01 pg/mL), which have previously been described as training agents [11]. As expected, upon secondary stimulation with LPS (10 ng/mL) on day 6, these cells produced more IL-6 and TNF- α compared to the untrained cells. However, they did not show increased levels of CXCL9 or CXCL11, and although they secrete CXCL10, the levels are lower compared to those induced by iSARS-CoV-2-trained monocytes (online suppl. Fig. 1; for all online suppl. material, see <https://doi.org/10.1159/000535120>).

Since one of the traits of trained innate cells is to respond stronger to unrelated stimuli, we incubated the iSARS-CoV-2-trained monocytes on day 6 with another nonspecific stimulus, namely, an inactivated preparation of the Gram-negative bacterium *B. pertussis* (MOI: 2). Findings indicate that iSARS-CoV-2-trained monocytes also produced sig-

nificant higher levels of IL-6 (1.3-fold), CXCL9 (1.9-fold), CXCL10 (4.2-fold), and CXCL11 (1.9-fold) and an increased trend of TNF- α (1.3-fold) in response to *B. pertussis* compared to untrained monocytes (shown in Fig. 3).

We then wanted to investigate whether this immune training is specific for SARS-CoV-2 or the effect of a single stranded RNA virus. To address this point, we used iH1N1 viral preparation at different MOI: 3, 1, 0.1, and the same protocol to induce training in monocytes from six healthy donors. No changes in the levels of secreted cytokines/chemokines were observed after restimulation with LPS on day 6. Indicating that the described training is specific for iSARS-CoV-2 and that using this in vitro model, iH1N1 did not induce trained immunity in monocytes (online suppl. Fig. 2).

iSARS-CoV-2 Induces a Distinct Gene Expression Profile of Trained Human Monocytes

The enhanced cytokine secretion by the iSARS-CoV-2-trained monocytes upon restimulation is one of the features indicative of trained immunity. In order to

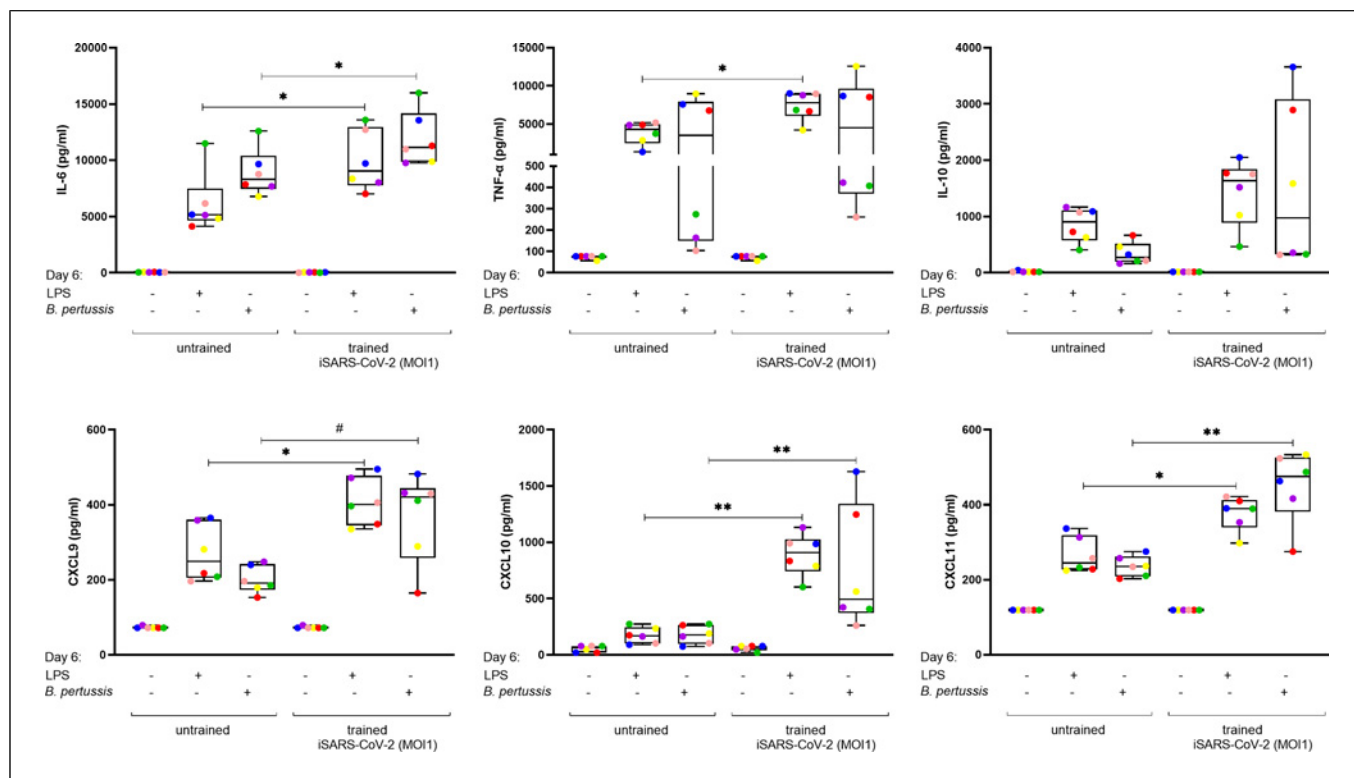


Fig. 3. Training of monocytes with iSARS-CoV-2 and rechallenged with nonspecific stimuli. Human monocytes were cultured in medium only or treated with iSARS-CoV-2 (MOI: 1) for 24 h followed by a washing step. After a resting period of 5 days, the cells were stimulated with LPS (10 ng/mL) or an inactivated *Bordetella pertussis* (MOI: 2) preparation. After 24 h, the levels of secreted cytokines and chemokines were quantified. Cells either

cultured in medium only or cultured in medium and stimulated with LPS on day 6 were used as controls. Two groups were compared using Wilcoxon-Mann-Whitney test (LPS-stimulated untrained with iSARS-CoV-2-trained monocytes or *B. pertussis* stimulated untrained with iSARS-CoV-2-trained monocytes). The results are expressed as the mean \pm SD ($n = 6$ from three independent experiments). * $p < 0.05$; ** $p < 0.01$; # ES < 0.7 .

explore other hallmarks of this process, we next examined the transcriptomic profile of iSARS-CoV-2-trained and -untrained monocytes prior to and after a secondary stimulation with LPS. Comparisons were made among four groups, namely, Unt-Med; Unt-LPS on day 6; Trn_S-Med without a second stimulus, and Trn_S-LPS on day 6. Principal component analysis of normalized and batch corrected read counts (shown in Fig. 4a) clearly separates in PC1 (25.28%), the Unt-LPS group from the other groups. PC2 (23.54%), on the other hand, separates the Trn_S-LPS group from the clusters representing cells without the addition of LPS on day 6 (Unt-Med and Trn_S-Med).

A heatmap representation of the top50 most variable DEGs between iSARS-CoV-2-trained versus -untrained monocytes after LPS stimulation is shown in Figure 4b. Addition of LPS to either the SARS-CoV-2-trained or -untrained cells resulted in an increased expression of several immune-related genes. However,

a clear difference in the gene expression profile between the SARS-CoV-2-trained and -untrained monocytes can be observed. The dendrogram on the left indicates three clusters (1, 2, and 3). Genes from two clusters, namely, 1 and 3, are highly expressed in the Trn_S-LPS group, whereas genes from cluster 2 are highly expressed in the Unt-LPS group of cells. Cluster 1 includes multiple genes encoding for cytokines (TNF and IFNB1), chemokines (CXCL3L1, CXCL9, CXCL10, CXCL11, CCL8, CCL20, and CCL3L1), genes associated with antigen presentation (HLA-DRB6), and genes induced by IFN α (IFI27). These findings corroborate our previous findings on increased secretion of TNF, CXCL9, CXCL10, CXCL11 by Trn_S-LPS monocytes. Cluster 2 includes genes encoding for various proinflammatory cytokines (IL-19, -24, -36G), chemokines (CCL2, CCL24, CXCL5), and a proinflammatory mediator (MMP12). Genes that belong to cluster 3 include those induced

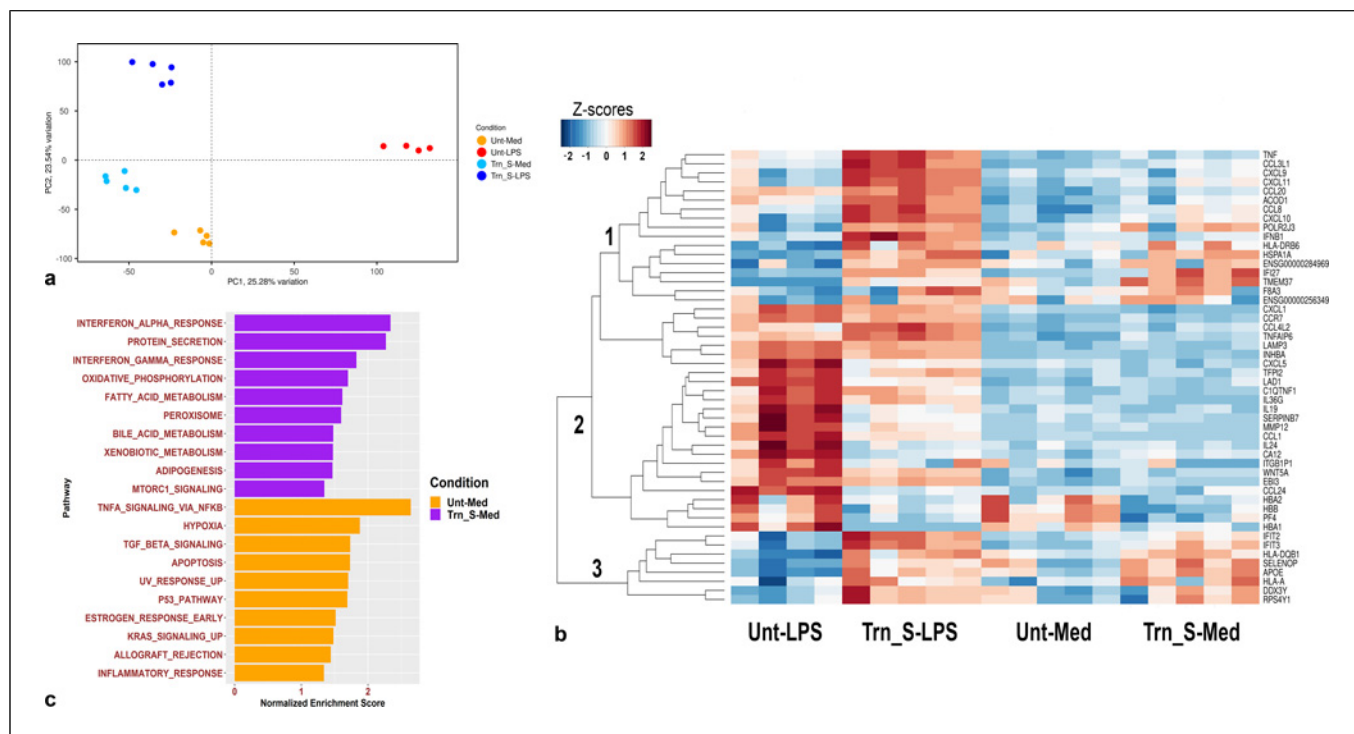


Fig. 4. Transcriptomic profiling of iSARS-CoV-2-trained monocytes. **a** Principal component analysis of normalized read counts corrected for batch and donor effect from untrained monocytes in medium only (Unt-Med); untrained monocytes stimulated with LPS on day 6 (Unt-LPS); trained monocytes with iSARS-CoV-2 without a second stimulus (Trn_S-Med), and iSARS-CoV-2-trained monocytes stimulated with LPS on day 6 (Trn_S-LPS). **b** Heatmap of the top 50 most variable DEGs between Trn_S-LPS and Unt-LPS. Gene expressions of these DEGs are also shown for

the trained and untrained cells without LPS (Unt-Med and Trn_S-Med). Colors from blue to red indicated low to high expression level in Z scores, respectively. ($p_{adj} < 0.05$, $\log_{2}FC > 1$ or < -1). **c** Pathway analysis of trained iSARS-CoV-2 cells without LPS restimulation (Trn_S-Med). Purple bars represent pathways enriched in Trn_S-Med, whereas orange bars represent enrichment in Unt-Med cells. The normalized enrichment score and false discovery rate (< 0.05) were calculated for each gene set using the Hallmark pathway database.

by IFN α (*IFIT2* and *IFIT3*), metabolic genes (*APOE* and *SELENOP*), and genes associated with antigen presentation (*HLADQB1* and *HLA-A*).

When analyzing the expression of these genes in the medium conditions (Unt-Med and Trn_S-Med), we observed a distinct profile for the trained monocytes (Trn_S-Med). This finding indicates that training with iSARS-CoV-2 already alters the gene expression profile of these cells even before the addition of the second stimulus. The genes upregulated in the SARS-CoV-2-trained cells in medium only belong to cluster 1 (*HLA-DRB6*, *IFI27*, and *TMEM37*, which encodes for a voltage-dependent calcium channel gamma-like subunit) and cluster 3 (*IFIT2*, *IFIT3*, *HLADQB1*, *APOE*, and *SELENOP*).

We next performed a pathway enrichment analysis to identify possible biological processes involved in the training of monocytes by iSARS-CoV-2. As expected, we observed that after LPS stimulation, pathways

associated with inflammatory immune responses were enriched (online suppl. Fig. 3). Noticeable is that these pathways were only enriched in the iSARS-CoV-2-trained compared to the untrained cells. However, when performing the pathway enrichment analysis on the cells without LPS stimulation, we observed that several of these inflammatory immune response pathways (interferon alpha and gamma response, as well as the TNF signaling) were also enriched in the iSARS-CoV-2-trained monocytes (shown in Fig. 4c). Other pathways enriched in the iSARS-CoV-2-trained monocytes include protein secretion and mTORC1 signaling. In addition, multiple pathways related to metabolism (fatty-acid metabolism, bile-acid metabolism, and xenobiotic-metabolism) were enriched. These findings indicate that besides a distinct proinflammatory response, changes in metabolism may be playing a role in monocyte training by iSARS-CoV-2.

Table 1. Significantly altered metabolic pathways in iSARS-CoV-2-trained monocytes (Trn_S-Med) compared to untrained monocytes (Unt-Med)

| Pathway | Pathway ID | <i>p</i> value | NES |
|---------------------------------------------------------------|------------|----------------|-------|
| Amino acid metabolism | WP3925 | 0.008 | 1.82 |
| Pyrimidine metabolism | WP4022 | 0.018 | 1.63 |
| Transsulfuration and one-carbon metabolism | WP2525 | 0.010 | 1.61 |
| Fatty acid biosynthesis | WP357 | 0.022 | 1.55 |
| Glycosaminoglycan degradation | WP4815 | 0.011 | 1.54 |
| Mitochondrial long-chain fatty acid beta-oxidation | WP368 | 0.014 | 1.54 |
| Glycosylation and related congenital defects | WP4521 | 0.016 | 1.53 |
| Oxysterols derived from cholesterol | WP4545 | 0.021 | 1.53 |
| Metabolic pathway of LDL, HDL, and TG, including diseases | WP4522 | 0.017 | 1.50 |
| Pathways of nucleic acid metabolism and innate immune sensing | WP4705 | 0.032 | 1.50 |
| One-carbon metabolism | WP241 | 0.026 | 1.49 |
| Cysteine and methionine catabolism | WP4504 | 0.033 | 1.46 |
| One-carbon metabolism and related pathways | WP3940 | 0.026 | 1.42 |
| Prostaglandin synthesis and regulation | WP98 | 0.041 | 1.41 |
| Estrogen metabolism | WP697 | 0.002 | -1.56 |
| Oxidation by cytochrome P450 | WP43 | 0.005 | -1.59 |
| Melatonin metabolism and effects | WP3298 | 0.011 | -1.61 |
| Tamoxifen metabolism | WP691 | 0.001 | -1.61 |
| Vitamin D receptor pathway | WP2877 | 0.001 | -1.65 |
| Tryptophan metabolism | WP465 | 0.002 | -1.67 |
| Vitamin D in inflammatory diseases | WP4482 | 0.001 | -1.71 |

Enrichment analysis with fgsea in R revealed 21 significant metabolic pathways ($p < 0.05$). 14 pathways are upregulated in trained cells (NES >0) and seven are downregulated (NES <0). NES, normalized enrichment score.

Metabolic Alterations Involved in the Training Effects of iSARS-CoV-2 on Monocytes

Since we found several differentially expressed metabolic genes in trained iSARS-CoV-2 monocytes, we decided to further explore how the metabolic pathways are affected. A pathway enrichment analysis was performed using the human pathway collection of WikiPathways to identify metabolic processes altered after training. When comparing trained (Trn_S-Med) and untrained (Unt-Med) monocytes without LPS, we identified 21 altered metabolic pathways, of which 14 are upregulated and seven are downregulated (shown in Table 1). These upregulated pathways are mainly related to amino acid metabolism, energy metabolism, and lipid metabolism. The detailed amino acid metabolism pathway model (WP3925) was explored visually to identify the molecular changes after training with iSARS-CoV-2. As shown in Figure 5, many genes belonging to amino acid metabolism (*MAOA*, *BCAT1*, *EHHADH*, *HADH*, *BCAT1*, *EHHADH*, *HIBCH*, *HBADH*, *HMGCL*), TCA cycle (*FH*, *IDH1*, *ACO2*, *OGDH*, *ACLY*, *SDHC*, *SDHD*, *SDHB*), glutamate metabolism (*GLUL*, *EPRS*, *GCLM*), glycolysis (*PKM*),

fatty acid biosynthesis (*FADS2*, *ELOVL4*, *ACOT2*, *ACL3*, *FADS1*, *SCD*), and cholesterol metabolism (*DCHR7*, *SC5D*) were upregulated.

Histone Methylation and Histone Acetylation Involved Training Effects of iSARS-CoV-2 on Monocytes

The epigenetic modifications are catalyzed by epigenetic enzymes: writers (add chemical modifications on DNA and histones) and erasers (remove chemical modifications on DNA and histones) [35]. When analyzing the gene expression profile of the iSARS-CoV-2-trained monocytes, we observed that many genes encoding for the writers such as a component of a histone methyltransferase complex (*SETDB2*), histone acetyltransferase-1 (*HAT1*), and protein arginine methyltransferase (*PRMT2*) were upregulated (shown in Fig. 6a). Since epigenetic modifications are one of the hallmarks of trained immunity, we examined the effect of inhibiting two well-known modifications, namely, histone acetylation and methylation, on human monocytes trained with iSARS-CoV-2. Previous studies have shown that both inhibition of a histone lysine methyltransferase

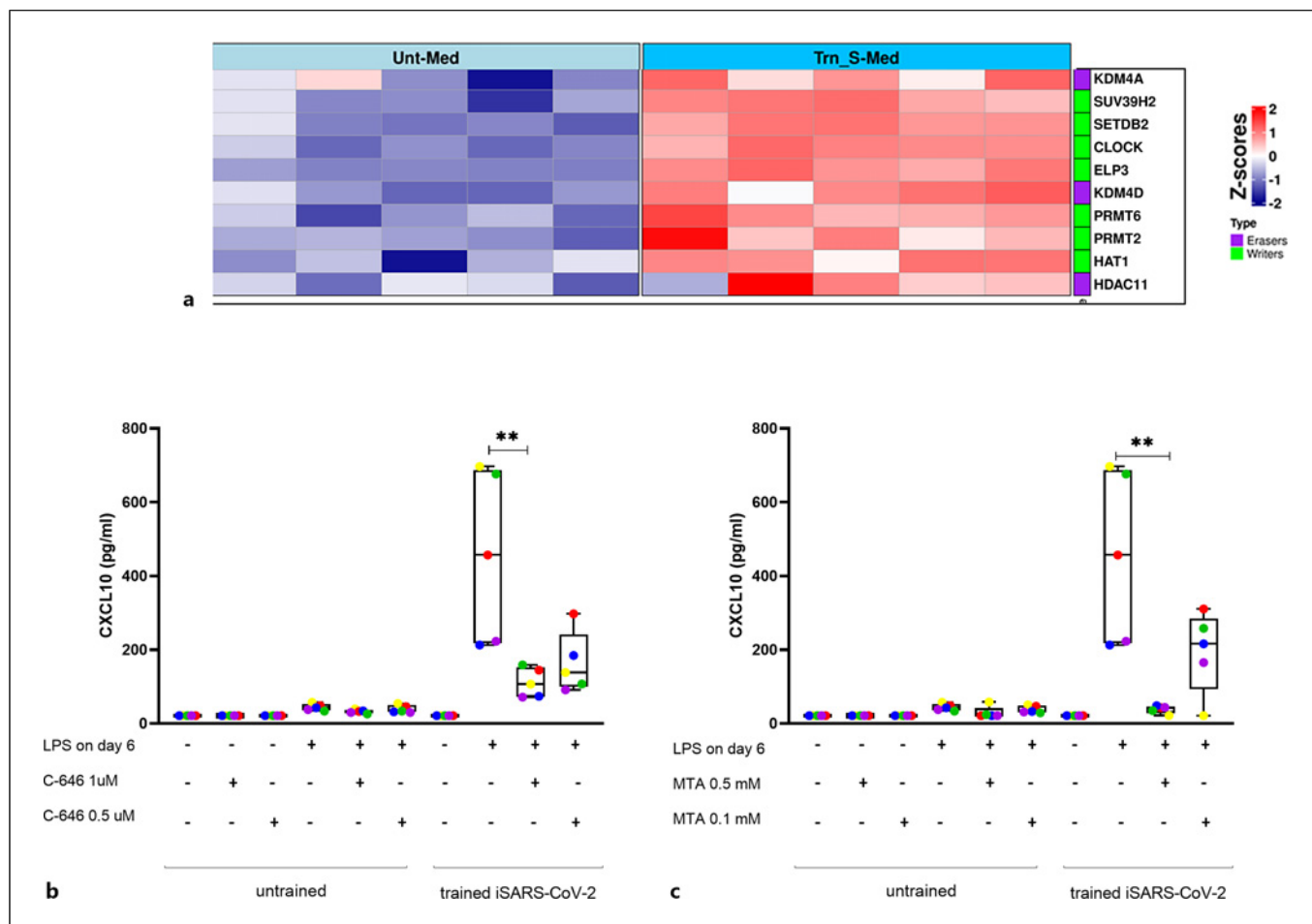


Fig. 6. Inhibition of histone acetylation or histone methylation interferes with the training effects induced by iSARS-CoV-2. **a** Heatmap of the most variable differentially expressed epigenetic genes between Trn_S-Med and Unt_Med. Colors from blue to red indicated low to high expression level in Z scores, respectively. **b, c** Human monocytes were pretreated with histone acetyltransferase inhibitor (C-646) or methyltransferase inhibitor (MTA) for 1 h prior to the treatment with iSARS-CoV-2 (MOI: 1) for 24 h. After washing and allowing them to

rest for the next 5 days, the cells were either stimulated on day 6 with LPS (10 ng/mL) or cultured in medium only. After 24 h, the concentration of CXCL10 was quantified. Groups were compared using the Kruskal-Wallis test followed by the Dunn's post-hoc test (LPS-stimulated trained monocytes with iSARS-CoV-2-trained monocytes pretreated with different inhibitor concentrations). The results are expressed as the mean \pm SD ($n = 5$ from two independent experiments). $**p < 0.01$.

Discussion

The present study shows that iSARS-CoV-2 induces trained immunity in human monocytes as indicated by changes in their transcriptomic, epigenetic, and metabolic profiles, as well as an enhanced inflammatory response to a nonspecific secondary stimulus. From titration experiments using different SARS-CoV-2 MOI, it was observed that only MOI: 1 induced training of human monocytes. Earlier studies have also reported that the functional fate of monocytes depends on the concentration of the pathogen-associated molecular patterns engaging the specific PRRs

[11]. Accordingly, different concentrations of the same PRR ligand can induce in time either tolerance (no response after restimulation) or training, by which the monocytes respond stronger to a second stimulus [11]. These different monocyte functionalities, induced by the same PRR ligand, are mediated by epigenetic mechanisms and play an essential role in either enhancing or preventing an excessive immune response upon secondary infection [38, 39]. For iSARS-CoV-2 induced trained immunity in monocytes, the PRRs involved remain to be determined.

When a nonspecific second stimuli such as LPS or the bacterial (*B. pertussis*) preparation were added to the

iSARS-CoV-2-trained monocytes, we observed that these cells secreted significantly higher levels of the proinflammatory cytokines and chemokines IL-6, TNF- α , CXCL9, CXCL10, and CXCL11 compared to untrained cells stimulated with the same nonspecific stimuli. These proinflammatory cytokines and chemokines have pleiotropic functions and have been described to be essential for protection in the infected host [7]. Although not significant, the iSARS-CoV-2-trained monocytes secreted after the second stimuli higher levels of the anti-inflammatory cytokine IL-10. This cytokine is also essential during an immune response to pathogens due to its role in suppressing exaggerated responses in order to prevent tissue damage [40]. Most of these cytokines and chemokines were also detected at the transcription level. Furthermore, among the top enriched pathways detected in the trained SARS-CoV-2 monocytes restimulated with LPS were those that belong to pro-inflammatory immune responses such as TNFA signaling via NF κ B, as well as the ones involving interferon alpha and gamma responses. Human monocytes have previously been shown to be trained in vitro with different training agents such as β -glucan, LPS, MDP (also used as controls in this study), uric acid, oxidized low-density lipoprotein, and the BCG vaccine. Our findings are consistent with other studies showing that training of monocytes with these agents results in increased secretion of cytokines such as IL-6 and TNF- α upon exposure to a second stimulus both at the protein and transcriptome levels [11–14].

One of the highlights of our data is the clear link between CXCL10 and trained immunity induced by iSARS-CoV-2. CXCL10 is also known as interferon-induced protein 10 (IP-10) and is secreted in response to IFN γ by various cells. Despite the lack of IFN γ detected in supernatants after secondary stimulation, CXCL10 was highly secreted by iSARS-CoV-2-trained monocytes, and much less by monocytes trained with other well-known agents in response to LPS. CXCL10 is an inflammatory chemokine that during infection acts as chemoattractant for other immune cells including macrophages, T cells, dendritic cells, and NK cells, which is essential for combating pathogens [41]. High levels of this chemokine can act as “friend or foe” since it has been reported to play an important role in viral clearance but also in disease pathogenesis [41]. In a recent study by Bergamaschi et al. [42], the authors reported on a heightened production of CXCL10, IL-15, and IFN γ in individuals immunized against COVID-19 with the BNT162b2 mRNA vaccine, which correlated with effective antiviral immune response. Interestingly, our study revealed that the iSARS-CoV-2-trained monocytes restimulated with LPS showed higher expression of IFN-stimulated genes.

In addition to measuring the secretion of cytokines/chemokines upon restimulation of iSARS-CoV-2-trained monocytes, we also investigated the expression of genes involved in other molecular processes which have been related to trained immunity such as metabolic and epigenetic remodeling [9]. The DEGs related to amino acid, energy, and lipid metabolism pathways were significantly enriched between iSARS-CoV-2-trained and -untrained monocytes. In line with our findings, a previous work has shown that innate immune memory is associated with the upregulation of several metabolic pathways that provide energy to cells after their activation. For example, a shift from oxidative phosphorylation to aerobic glycolysis was observed in trained monocytes by β -glucan [6, 38]. Also, glycolysis and glutamine metabolism are crucial for trained monocytes induced by BCG [43]. These shifts in metabolism are mediated through the Akt/mTOR (mammalian target of rapamycin)/HIF1 α (hypoxia-inducible factor 1 α) pathway [6, 38, 43], and inhibition of this pathway prevents trained immunity [43]. This is in line with our findings where mTORC1 signaling is also upregulated in iSARS-CoV-2-trained monocytes. In addition to glycolysis and glutamine metabolism, upregulation of cholesterol and fatty acid synthesis plays an important role in innate immune memory. Bekkering et al. [44] found that the inhibition of the cholesterol synthesis pathway abolished trained immunity in monocytes induced by β -glucan, and intracellular mevalonate is crucial for inducing trained immunity. Interestingly, in addition to the abovementioned pathways, we detected changes in the expression of genes related to the vitamin D signaling pathway. The role of vitamin D in trained immunity is not known yet but it has been described to have an important role in immunomodulation, including in COVID-19 [45]. Furthermore, we found that many genes belonging to the TCA cycle were upregulated. One of the functions of this cycle is ATP synthesis but it can also provide metabolites which serve as cofactors for epigenetic enzymes and consequently, it plays a role in the regulation of inflammatory response during innate immune memory [46]. For example, both fumarate and succinate increase global histone methylation [47] and citrate is used to produce acetyl-CoA, which is a substrate for histone acetyltransferase [48].

Histone modifications (histone methylation and acetylation) have been reported to be essential in trained immunity. Trimethylation of histone 3 lysine 4 (H3K4me3) and acetylation of histone 3 lysine 27 (H3K27ac) are two important epigenetic markers of active promoters and enhancers associated with gene expression and innate immune memory. H3K4me3 and H3K27ac modifications have been observed in trained monocytes by BCG or β -glucan [5–7]. Here, we observed that the iSARS-CoV-2-trained cells have increased

the expression of genes encoding the writers compared to the erasers such as *SETDB2* associated with H3K4me3, *HAT1* is involved in histone acetylation particularly of histone H4 and *PRMT2* involved in several process including histone methylation [35]. These findings suggest that epigenetic changes take place in iSARS-CoV-2-trained monocytes. Although the exact epigenome remains to be determined, our study shows that blocking the histone methyltransferases or histone acetyltransferases diminished the training effects of iSARS-CoV-2 on monocytes, indicating that these modifications play a significant role in the trained immunity process induced by this viral preparation. Our observation is in line with other studies which also demonstrated that trained immunity in monocytes induced by β -glucan, MDP, or flagellin is almost completely abolished by blocking histone methyltransferases or histone acetyltransferases [11]. Inhibition of histone methyltransferases has been also shown by others to almost abolish the innate immune memory in BCG-trained monocytes [14] or in cells trained by *Fasciola hepatica* total extract [49].

Using clinical samples, others have suggested that trained immunity is induced in convalescent COVID-19 patients [20, 21] or after vaccination with the adenoviral vector-based COVID-19 vaccine [18]. Indeed, our in vitro model confirms that SARS-CoV-2 can train human monocytes by rewiring the cell metabolism and epigenetic processes to respond stronger to a second stimulus. Whether live SARS-CoV-2 and COVID-19 vaccines also induce trained immunity in human monocytes could be investigated using the in vitro model here described. Although the duration and effect of trained immunity on long-term protection are still unclear, our data contribute to the knowledge required to further optimize (COVID-19) vaccination strategies to prevent and control infectious diseases.

Acknowledgment

The authors thank Jørgen de Jonge from the Center for Infectious Disease Control (National Institute for Public Health and the Environment, the Netherlands) for providing the inactivated SARS-CoV-2 and H1N1 preparations.

References

- 1 Qi H, Liu B, Wang X, Zhang L. The humoral response and antibodies against SARS-CoV-2 infection. *Nat Immunol*. 2022;23(7):1008–20.
- 2 Sette A, Crotty S. Immunological memory to SARS-CoV-2 infection and COVID-19 vaccines. *Immunol Rev*. 2022;310(1):27–46.
- 3 Netea MG, Quintin J, van der Meer JWM. Trained immunity: a memory for innate host defense. *Cell Host Microbe*. 2011;9(5):355–61.
- 4 Kleinnijenhuis J, Quintin J, Preijers F, Benn CS, Joosten LAB, Jacobs C, et al. Long-lasting effects of BCG vaccination on both heterologous Th1/Th17 responses and innate trained immunity. *J Innate Immun*. 2014;6(2):152–8.
- 5 Bekkering S, Domínguez-Andrés J, Joosten LAB, Riksen NP, Netea MG. Trained immunity: reprogramming innate immunity in Health and disease. *Annu Rev Immunol*. 2021;39(1):667–93.

Statement of Ethics

This study was conducted according to the principles described in the Declaration of Helsinki. Buffy coats were from healthy adult Dutch Blood Bank donors participating in a Not-For-Transfusion study registered under protocol NVT0201.01 (Sanquin, The Netherlands). All blood donors provided written informed consent for blood collection and subsequent analyses. Blood samples were processed anonymously and the research goal, primary cell isolation, required no review by an accredited Medical Research Ethics Committee, as determined by the Dutch Central Committee on Research involving human subjects.

Conflict of Interest Statement

The authors declare no commercial relationships that might pose a conflict of interest in connection with the submitted manuscript.

Funding Sources

This study was funded by the Dutch Ministry of Health, Welfare, and Sport (VWS), The Netherlands.

Author Contributions

J.C. and E.P. participated in the design of study and wrote the manuscript; J.C. and R.H.J.J. performed the experiments; J.G. participated in RNAseq experiments; A.M.-B., J.C., E.P., M.K., N.P., and vdG.M.D.B. participated in data analysis and interpretation; vdG.M.D.B. edited and reviewed the manuscript; and E.P. supervised the study. All authors read and approved the final manuscript.

Data Availability Statement

All data used for the analysis in this study are available. Further inquiries can be directed to the corresponding author. All RNAseq data are available in the GEO database, accession number: GSE235094.

- 6 Cheng SC, Quintin J, Cramer RA, Shephardson KM, Saeed S, Kumar V, et al. mTOR and HIF-1 α -mediated aerobic glycolysis as metabolic basis for trained immunity. *Science*. 2014;345(6204):1250684.
- 7 Arts RJW, Moorlag SJCFM, Novakovic B, Li Y, Wang SY, Oosting M, et al. BCG vaccination protects against experimental viral infection in humans through the induction of cytokines associated with trained immunity. *Cell Host Microbe*. 2018;23(1):89–100.e5.
- 8 Cirovic B, de Bree LCJ, Groh L, Blok BA, Chan J, van der Velden WJFM, et al. BCG vaccination in humans elicits trained immunity via the hematopoietic progenitor compartment. *Cell Host Microbe*. 2020;28(2):322–34.e5.
- 9 Riksen NP, Netea MG. Immunometabolic control of trained immunity. *Mol Aspects Med*. 2021;77:100897.
- 10 Ferreira AV, Domínguez-Andrés J, Netea MG. The role of cell metabolism in innate immune memory. *J Innate Immun*. 2022;14(1):42–50.
- 11 Ifrim DC, Quintin J, Joosten LAB, Jacobs C, Jansen T, Jacobs L, et al. Trained immunity or tolerance: opposing functional programs induced in human monocytes after engagement of various pattern recognition receptors. *Clin Vaccine Immunol*. 2014;21(4):534–45.
- 12 Bekkering S, Blok BA, Joosten LAB, Riksen NP, van Crevel R, Netea MG. *Vitro* experimental model of trained innate immunity in human primary monocytes. *Clin Vaccine Immunol*. 2016;23(12):926–33.
- 13 Cabău G, Crișan TO, Klück V, Popp RA, Joosten LAB. Urate-induced immune programming: consequences for gouty arthritis and hyperuricemia. *Immunol Rev*. 2020;294(1):92–105.
- 14 Kleinnijenhuis J, Quintin J, Preijers F, Joosten LAB, Ifrim DC, Saeed S, et al. Bacille Calmette-Guérin induces NOD2-dependent nonspecific protection from reinfection via epigenetic reprogramming of monocytes. *Proc Natl Acad Sci U S A*. 2012;109(43):17537–42.
- 15 Wimmers F, Donato M, Kuo A, Ashuach T, Gupta S, Li C, et al. The single-cell epigenomic and transcriptional landscape of immunity to influenza vaccination. *Cell*. 2021;184(15):3915–35.e21.
- 16 Ziogas A, Netea MG. Trained immunity-related vaccines: innate immune memory and heterologous protection against infections. *Trends Mol Med*. 2022;28(6):497–512.
- 17 Li C, Lee A, Grigoryan L, Arunachalam PS, Scott MKD, Trisal M, et al. Mechanisms of innate and adaptive immunity to the Pfizer-BioNTech BNT162b2 vaccine. *Nat Immunol*. 2022;23(4):543–55.
- 18 Arunachalam PS, Scott MKD, Hagan T, Li C, Feng Y, Wimmers F, et al. Systems vaccinology of the BNT162b2 mRNA vaccine in humans. *Nature*. 2021;596(7872):410–6.
- 19 Murphy DM, Cox DJ, Connolly SA, Breen EP, Brugman AAI, Phelan JJ, et al. Trained immunity is induced in humans after immunization with an adenoviral vector COVID-19 vaccine. *J Clin Invest*. 2023;133(2):e162581.
- 20 You M, Chen L, Zhang D, Zhao P, Chen Z, Qin EQ, et al. Single-cell epigenomic landscape of peripheral immune cells reveals establishment of trained immunity in individuals convalescing from COVID-19. *Nat Cell Biol*. 2021;23(6):620–30.
- 21 Utrero-Rico A, González-Cuadrado C, Chivite-Lacaba M, Cabrera-Marante O, Laguna-GoyaAlmendo-Vazquez RP, Almendo-Vázquez P, et al. Alterations in circulating monocytes predict COVID-19 severity and include chromatin modifications still detectable six months after recovery. *Biomedicines*. 2021;9(9):1253.
- 22 van de Ven K, van Dijken H, Wijsman L, Gomersbach A, Schouten T, Kool J, et al. Pathology and immunity. After SARS-CoV-2 infection in male ferrets is affected by age and inoculation route. *Front Immunol*. 2021;12:750229.
- 23 van de Ven K, de Heij F, van Dijken H, Ferreira JA, de Jonge J. Systemic and respiratory T-cells induced by seasonal H1N1 influenza protect against pandemic H2N2 in ferrets. *Commun Biol*. 2020;3(1):564.
- 24 Kroes MM, Miranda-Bedate A, Hovingh ES, Jacobi R, Schot C, Pupo E, et al. Naturally circulating pertactin-deficient Bordetella pertussis strains induce distinct gene expression and inflammatory signatures in human dendritic cells. *Emerg Microbes Infect*. 2021;10(1):1358–68.
- 25 Bray NL, Pimentel H, Melsted P, Pachter L. Near-optimal probabilistic RNA-seq quantification. *Nat Biotechnol*. 2016;34(5):525–7.
- 26 Sergushichev AA, Loboda AA, Jha AK, Vincent EE, Driggers EM, Jones RG, et al. GAMT: a web-service for integrated transcriptional and metabolic network analysis. *Nucleic Acids Res*. 2016;44(W1):W194–200.
- 27 Wickham H. *Ggplot2: elegant graphics for data analysis*. Cham, Switzerland: Springer International Publishing; 2016. p. 1–260.
- 28 Subramanian A, Tamayo P, Mootha VK, Mukherjee S, Ebert BL, Gillette MA, et al. Gene set enrichment analysis: a knowledge-based approach for interpreting genome-wide expression profiles. *Proc Natl Acad Sci U S A*. 2005;102(43):15545–50.
- 29 Liberzon A, Birger C, Thorvaldsdóttir H, Ghandi M, Mesirov JP, Tamayo P. The Molecular Signatures Database (MSigDB) hallmark gene set collection. *Cell Syst*. 2015;1(6):417–25.
- 30 Martens A, Ammar A, Riutta A, Waagmeester M, Slenter D, Hanspers K, et al. WikiPathways: connecting communities. *Nucleic Acids Res*. 2021;49(D1):D613–21.
- 31 Shannon P, Markiel A, Ozier O, Baliga NS, Wang JT, Ramage D, et al. Cytoscape: a software environment for integrated models of biomolecular interaction networks. *Genome Res*. 2003;13(11):2498–504.
- 32 Kutmon M, Lotia S, Evelo CT, Pico AR. WikiPathways App for Cytoscape: making biological pathways amenable to network analysis and visualization. *F1000Res*. 2014;3:152.
- 33 Cliff N. Dominance statistics: ordinal analyses to answer ordinal questions. *Psychol Bull*. 1993;114(3):494–509.
- 34 Vargha A, Delaney HD, Vargha A. A critique and improvement of the “CL” common language effect size statistics of McGraw and Wong. *J Educ Behav Stat*. 2000;25(2):101–32.
- 35 Biswas S, Rao CM. Epigenetic tools (The Writers, the Readers and the Erasers) and their implications in cancer therapy. *Eur J Pharmacol*. 2018;837:8–24.
- 36 Gu Y, Wang X, Liu H, Li G, Yu W, Ma Q. SET7/9 promotes hepatocellular carcinoma progression through regulation of E2F1. *Oncol Rep*. 2018;40(4):1863–74.
- 37 van den Bosch T, Boichenko A, Leus NGJ, Ourailidou ME, Wapenaar H, Rotili D, et al. The histone acetyltransferase p300 inhibitor C646 reduces pro-inflammatory gene expression and inhibits histone deacetylases. *Biochem Pharmacol*. 2016;102:130–40.
- 38 Saeed S, Quintin J, Kerstens HHD, Rao NA, Aghajani-refah A, Matarese F, et al. Epigenetic programming of monocyte-to-macrophage differentiation and trained innate immunity. *Science*. 2014;345(6204):1251086.
- 39 Divangahi M, Aaby P, Khader SA, Barreiro LB, Bekkering S, Chavakis T, et al. Trained immunity, tolerance, priming and differentiation: distinct immunological processes. *Nat Immunol*. 2021;22(1):2–6.
- 40 Rojas JM, Avia M, Martín V, Sevilla N. IL-10: a multifunctional cytokine in viral infections. *J Immunol Res*. 2017;2017:6104054.
- 41 Elemam NM, Talaat IM, Maghazachi AA. CXCL10 chemokine: a critical player in RNA and DNA viral infections. *Viruses*. 2022;14(11):2445.
- 42 Bergamaschi C, Terpos E, Rosati M, Angel M, Bear J, Stellas D, et al. Systemic IL-15, IFN- γ , and IP-10/CXCL10 signature associated with effective immune response to SARS-CoV-2 in BNT162b2 mRNA vaccine recipients. *Cell Rep*. 2021;36(6):109504.
- 43 Arts RJW, Carvalho A, La Rocca C, Palma C, Rodrigues F, Silvestre R, et al. Immunometabolic pathways in BCG-induced trained immunity. *Cell Rep*. 2016;17(10):2562–71.
- 44 Bekkering S, Arts RJW, Novakovic B, Kourtzelis I, van der Heijden CDCC, Li Y, et al. Metabolic induction of trained immunity through the mevalonate pathway. *Cell*. 2018;172(1–2):135–46.e9.

- 45 Xu Y, Baylink DJ, Chen CS, Reeves ME, Xiao J, Lacy C, et al. The importance of vitamin d metabolism as a potential prophylactic, immunoregulatory and neuroprotective treatment for COVID-19. *J Transl Med*. 2020;18(1):322.
- 46 Ryan DG, O'Neill LAJ. Krebs cycle reborn in macrophage immunometabolism. *Annu Rev Immunol*. 2020;38:289–313.
- 47 Sun L, Zhang H, Gao P. Metabolic reprogramming and epigenetic modifications on the path to cancer. *Protein Cell*. 2022; 13(12):877–919.
- 48 Friedmann DR, Marmorstein R. Structure and mechanism of non-histone protein acetyltransferase enzymes. *FEBS J*. 2013;280(22): 5570–81.
- 49 Quinn SM, Cunningham K, Raverdeau M, Walsh RJ, Curham L, Malara A, et al. Anti-inflammatory trained immunity mediated by helminth products attenuates the induction of T cell-mediated auto-immune disease. *Front Immunol*. 2019;10: 1109.